Wide bandwidth, large, and tunable polarization mode dispersions in multilayered omnidirectional reflectors

Zheng Wang
Department of Applied Physics, Stanford University, Stanford, California 94305

David A. B. Miller and Shanhui Fan[a)]
Department of Electrical Engineering, Stanford University, Stanford, California 94305

(Received 4 March 2002; accepted for publication 9 May 2002)

We numerically demonstrate the generation of large, broadband, and tunable polarization mode dispersion (PMD) with omnidirectionally reflecting dielectric stacks with embedded cavities. Both first-order and second-order polarization mode dispersion can be generated by similar configurations. Our examples show that the first-order PMD can be tuned from 0 to 30 ps over an 80 GHz bandwidth and second-order PMD from 0 to 50 ps/nm can be generated over a 100 GHz bandwidth. We also show that in our configuration there is no significant modal distortion of the light beams when the beam diameters exceed 3.5 mm. © *2002 American Institute of Physics.* [DOI: 10.1063/1.1491284]

Polarization mode dispersion (PMD) is a critical bandwidth-limiting issue for ultrahigh data rate communication systems using installed optical fiber links and for long-distance high-speed fiber links in general.[1–6] Cabled fibers show time-varying PMD due to manufacturing imperfections, stress, and ambient temperature changes. Adaptive compensation is therefore necessary. The first-order PMD results from the differential group delay between the two principal states of polarizations in the fibers, while the differential chromatic dispersion between polarizations generates second-order PMD. To achieve adaptive compensation at each order, it is essential to provide components with sufficient operation bandwidth that can generate large and tunable differential group delay and differential chromatic dispersion.

Previously, adaptive first-order PMD compensation techniques have typically used configurations with beam splitters and separate tunable fiber-delay lines.[1–6] These devices usually suffer from relatively large insertion loss, low tuning speed, and large physical dimensions. Moreover, second-order PMD cannot be easily compensated with such configurations. In this letter, based upon the recently discovered effect of omnidirectional reflection in dielectric multilayer mirrors, we introduce a class of structures that can generate both the first-order and the second-order PMD with large bandwidth and low insertion loss. In addition, we show that the tuning of the device can be realized by a simple angular tuning scheme. The large PMD in this design may enable it to replace the bulky fiber delay lines in current technology.

The basic building block of our design consists of a microcavity layer sandwiched between two omnidirectional reflectors [Fig. 1(a)]. An omnidirectional reflector is a periodic multilayer dielectric stack that possesses near 100% reflectivity within a range of frequencies, regardless of incidence angles and polarizations.[7] Here for concreteness, we consider such reflectors made up of Si/SiO_2 bilayers. An extra layer of SiO_2 is embedded as the cavity. The cavity is configured in ''all-pass filter'' geometry: the reflector on one side of the cavity, on which the light is incident, possesses far larger transmissivity than the reflector on the other side. (This geometry is also commonly referred to as the Gires–Tournois interferometer,[8] and has been previously used in chromatic dispersion compensation.[9]) In this all-pass filter geometry, the intensity response function becomes independent from the phase response function, allowing for generation of rich varieties of phase response with low insertion loss.

For such a cavity structure, the spectra for reflectivity and group delay are calculated using the characteristic matrix method,[10] and shown in Figs. 1 and 2. Omni-directional reflection occurs within the wavelength range between 1250 and 1700 nm (Fig. 1). The presence of the cavity, while having little effect in the reflectance response function inside the photonic band gap, nevertheless introduces a large Lorentzian peak in the group delay spectrum (Fig. 2). At the normal incidence, the group delay peaks of the two polarizations coincide with each other, as expected. At off-normal incidence angles, the peaks shift to shorter wavelengths and split between the polarizations, resulting in a differential group delay. For practical applications, however, to prevent generation of higher-order PMD's, it is crucial to obtain flat delay spectra over a sufficiently large bandwidth that can cover a signal band, and maintain such flat spectra during the tuning process.

For a single cavity structure, there is an inherent trade-off between the maximum delay and the usable bandwidth. Therefore, we utilize an incoherent cascading scheme with multiple stages, as shown in Fig. 3(a). Each stage comprises two parallel dielectric stack single-cavity reflectors. These reflectors are arranged at a sufficient distance apart, for example a few centimeters, such that no interference occurs between reflections. Thus, the dispersive coefficients of the entire stage become the linear summation of those of individual reflections. Thus, larger group delay can be implemented without sacrificing bandwidth. In addition, the delay spectra of each stage can be tuned independently if needed. We show in Fig. 3 an example of a three-stage reflector

a)Electronic mail: shanhui@stanford.edu.

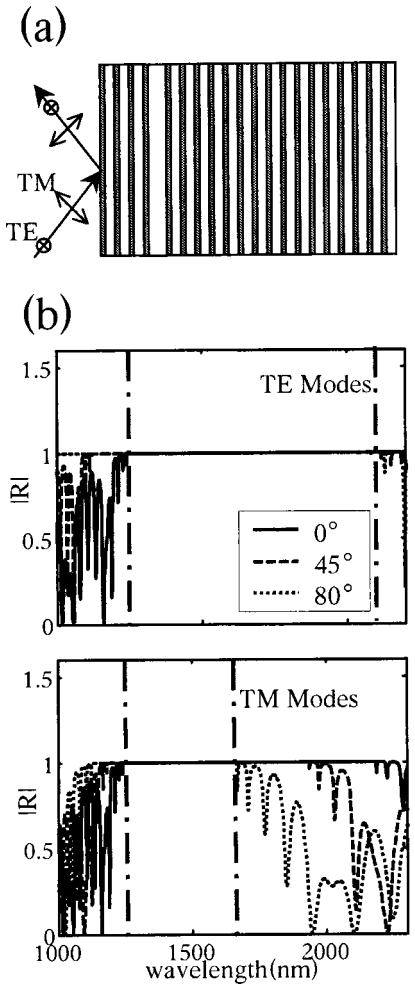

FIG. 1. (a) Cross section of a dielectric stack with an embedded microcavity. (b) Reflectance spectra for TE and TM modes at various incidence angles. A TE (TM) mode has its electric (magnetic) field parallel to the mirror surface. The frequency range between dashed lines corresponds to the range of omnidirectional reflectance. This range extends from 1250 to 1700 nm.

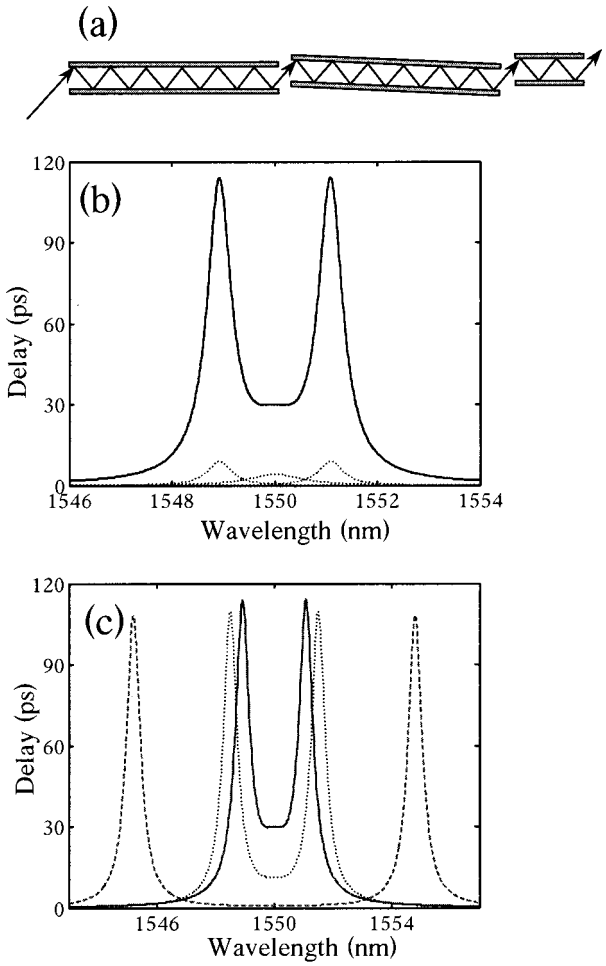

FIG. 3. (a) Schematic of a tunable differential group delay generator. The structure consists of three stages. Each stage is made up of two parallel reflectors. (b) The solid line corresponds to the aggregate delay spectrum of the structure. The dotted lines are the delay from a single reflection event in each stage. (c) Tuning of the aggregate delay as incident angle is varied. The maximum-rotational angle for the first two stages is 1.6° around an incidence angle of 30°.

incoherently cascaded. The first two stages, both with 12 reflections, generate two large differential group delay resonant peaks each with a Q of 3000, centered on either side of the 1550 nm signal band. The differential group delay at the signal band is consequently determined by the spacing between these two peaks. For adaptive tuning, each peak can be conveniently shifted by rotating the corresponding stage along the axes normal to the shared incident plane. Moreover, the even number of reflections at each stage ensures that the output light remains parallel to the input light, which eases the alignment between stages. A supplementary third stage with only four reflections is used to further flatten the spectra in the case of large delay when the two peaks are close to each other as shown in Fig. 3. This stage has a smaller Q of 1000 and a resonant frequency centered at the signal band. For lower differential group delays, this stage can be disabled by simply rotating it by a large angle so that the resonant peak is far from the signal band, and reflections in this stage do not accrue differential group delay. Using such a configuration, our simulation shows that a 0–30 ps differential group delay can be continuously tuned over an 80 GHz signal band centered at the wavelength of 1550 nm.

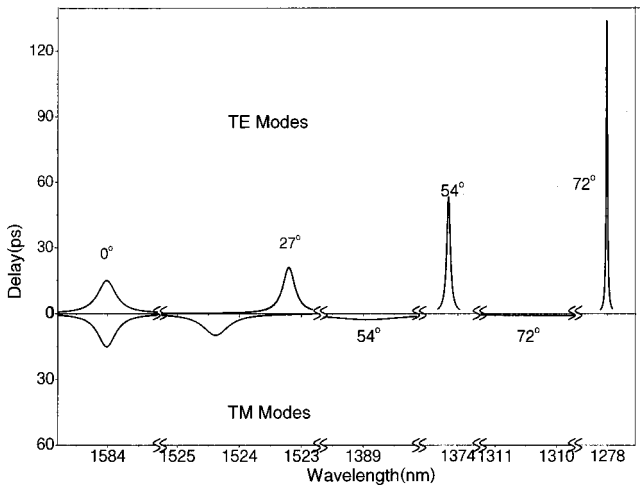

FIG. 2. Delay spectra at different incident angles for the dielectric stack shown in Fig. 1(a).

The flexibility of these angular tuning schemes further enables generation of a tunable second-order PMD. A similar three-stage system is used as in the first-order case, except that the two first stages are now aligned in such a way that

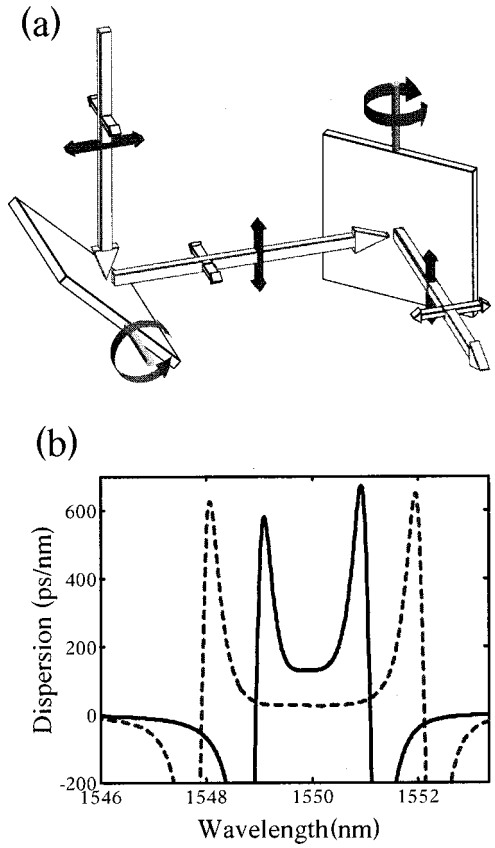

FIG. 4. (a) Schematic for a tunable second-order PMD generator. The two arrows represent the two principal states of polarization in the incoming signal. The polarization state represented by the outlined arrows is a TE mode with respect to the first mirror, and a TM mode with respect to the second mirror. The opposite holds true for the polarization state depicted by the solid arrow. (b) Differential chromatic dispersion response of a configuration similar to Fig. 3(a), except that the first two stages are connected in such a way as shown in Fig. 4(a). In each of the first two stages, there are 12 reflections events. The supplementary third stage further flattens the dispersion at high dispersion cases, similar to the case in Fig. 3(a).

each is parallel to one of the two orthogonal polarizations, as shown in Fig. 4(a). In this way, the overall differential group delay response becomes the difference of the two resonant peaks and is linear as a function of frequency between peaks. As a result, a constant differential chromatic dispersion occurs at the signal band between the two peaks. Similar to the first-order PMD compensation scheme, adjusting the spacing between the two resonant peaks by angular tuning result in tuning of the magnitude of the differential chromatic dispersion at the signal band, as illustrated in Fig. 3(b). The third low-Q supplementary stage can further flatten the spectra in the case of large differential chromatic dispersion as well. The orientation of the reflectors being the only difference with the first-order case, similar control schemes apply. Our numerical simulations indicate that a flat differential chromatic dispersion over 100 GHz bandwidth can be continuously tuned from 0 to 50 ps/nm, as illustrated in Fig. 5. For larger bandwidth, the maximum dispersion of single reflection has to be reduced and more reflections are therefore needed.

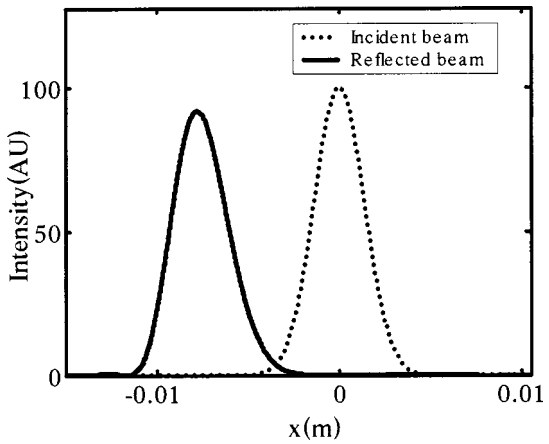

FIG. 5. Changes in the beam shape, as it goes through the structure shown in Fig. 3(a) after 28 reflections.

For any technique involving thin film structures at oblique incidence, the spatial distortion of the output beams has to be carefully considered to avoid coupling loss. Here, in both first and second-order cases, we specifically position the signal band in a fairly flat spectral range away from the resonant frequency. Because the variation of phase occurs relatively slowly over the signal band, the spatial distortion of beams is greatly reduced. This is in contrast with a naïve way to generate delay by placing the signal band at the resonance, which would incur severe spatial distortion for narrow beams as the phase varies significantly in the vicinity of the resonance. Simulations, as shown in Fig. 5, indicate that no significant distortion occurs for an incident beam with diameter of greater than 3.5 mm, and for the 0–30 ps tunable deferential group delay component mentioned earlier. The split between the two polarizations can be restored readily with a polarization beam splitter afterwards.

Finally, we note that these structures possess additional important advantages such as fast response speed and wide wavelength tracking range. For example, a differential group delay tuning from 0.5 to 30 ps corresponds to a rotation of the two main stages by only 1.7°. The small angle simplifies the control scheme and increases the potential response speed of the PMD compensator, which is critical for real-time adaptive applications. The use of omnidirectional reflector also greatly simplifies the reflector design at large incidence angles and assures a wide wavelength tracking range over 200 nm.

This work was supported in part by the Center for Integrated Systems at Stanford University, the NSF award No. ECS-0200445, and a 3M untenured faculty award.

[1] H. Rosenfeldt, R. Ulrich, U. Feiste, R. Ludwig, H. G. Weber, and A. Ehrhardt, Electron. Lett. **36**, 448 (2000).
[2] H. Y. Pua, K. Peddanarappagari, B. Zhu, C. Allen, K. Demarest, and R. Hui, J. Lightwave Technol. **18**, 832 (2000).
[3] D. Sobiski, D. Pikula, J. Smith, C. Henning, D. Chowdhury, E. Murphy, E. Kolltveit, and F. Annunziata, Electron. Lett. **37**, 46 (2001).
[4] C. K. Madsen, Opt. Lett. **25**, 878 (2000).
[5] E. Iannone, F. Matera, A. Mecozzi, and M. Settembre, *Nonlinear Optical Communication Networks*, (J Wiley, New York, 1998).
[6] Q. Yu, L.-S. Yan, Y. Xie, M. Hauer, and A. E. Wilner, IEEE Photonics Technol. Lett. **13**, 863 (2001).
[7] Y. Fink, J. N. Winn, S. Fan, C. Chen, J. Michel, J. D. Joannopoulos, and E. L. Thomas, Science **282**, 5394 (1998).
[8] F. Gires and P. Tournois, C. R. Acad. Sci. Paris **258**, 6112 (1964).
[9] M. Jablonski, Y. Tanaka, H. Yaguchi, K. Furuki, K. Sato, N. Higashi, and K. Kikuchi, IEEE Photonics Technol. Lett. **13**, 1188 (2001).
[10] M. Born and E. Wolf, *Principles of Optics* (Pergamon, Oxford, 1980).